



Research Article

Thermal analysis of Ag-water nanofluid flow induced by a horizontally stretching cylinder with electrified nanoparticles

Aditya Kumar PATI^{1,*} , Ashok MISRA¹ , Saroj Kumar MISHRA¹ 

¹Department of Mathematics, Centurion University of Technology and Management, Odisha, 761211, India

ARTICLE INFO

Article history

Received: 02 March 2024

Revised: 26 April 2024

Accepted: 26 August 2024

Keywords:

Electrified Nanoparticles; Mass

Transfer; MATLAB bvp4c;

Nanofluid; Thermal Analysis

ABSTRACT

Nanofluid flow over a stretching cylinder with the electrification effect of nanoparticles has sparked renewed industrial interest in applications like thermal insulation, metal spinning, liquid film condensation, and wire coating. To elevate process quality standards in these areas, the associated transport phenomena require ongoing advancements. Hence, the current study investigates the thermal and numerical aspects of the axisymmetric boundary layer flow of Ag-water nanofluid around a horizontally stretching cylinder. The combined effects of electrified nanoparticles and viscous dissipation on the flow of Ag-water nanofluid around a stretching cylinder remain unexplored in the existing literature. Hence, the present study considers nanoparticle electrification and viscous dissipation effects, which are often overlooked in conventional nanofluid models like Buongiorno's model. The study emphasizes the importance of nanoparticle electrification, especially in scenarios involving tribo-electrification due to Brownian motion. This unique aspect sets this investigation apart. The governing partial differential equations are transformed into local similarity equations using similarity transformations and nondimensionalization. The system of local similarity equations is then solved numerically using the MATLAB bvp4c solver. The results closely match those reported in previous studies. The study explores the effects of the Eckert number and electrification parameter on non-dimensional concentration, velocity, temperature, as well as heat and mass transfer coefficients through graphical analysis. The main finding highlighted in this study is the enhanced heat and mass transfer rates from a stretching cylinder to a nanofluid, facilitated by the presence of electrified nanoparticles. The electrified nanoparticle mechanism in nanofluids boosts heat transfer, benefiting manufacturing industries with high-temperature cylindrical products. This mechanism also enhances transport properties, improving drug delivery in biomedical applications. Moreover, the proposed model holds potential for applications in manufacturing and industrial cooling processes..

Cite this article as: Pati AK, Misra A, Mishra SK. Thermal analysis of Ag-water nanofluid flow induced by a horizontally stretching cylinder with electrified nanoparticles. Sigma J Eng Nat Sci 2025;43(4):1152–1165.

*Corresponding author.

*E-mail address: adityamathematics100@gmail.com

This paper was recommended for publication in revised form by Editor-in-Chief Ahmet Selim Dalkilic



INTRODUCTION

Recent advancements in nanotechnology have significantly broadened the scope of research for scientists and researchers. This is primarily due to the improved thermophysical properties and the extensive engineering and industrial applications offered by nanomaterials. The significance of these materials lies in their diverse applications across vehicle thermal management, solar energy systems, electronics cooling, fusion control, material processing industries and biomedical technologies. Nanofluids are liquid mixtures where nano-sized solid particles are dispersed within base liquids. Recent studies have focused on examining the transfer of heat and mass in situations involving the flow of nanofluids. These nanofluids, used in various industrial processes such as cooling in heat exchangers, microelectronics, and engine cooling, have attracted considerable attention for their ability to transfer heat efficiently. Additionally, nanofluids have applications in biomedical fields like cancer treatment and drug diffusion in the bloodstream. The use of nanofluids to improve heat transfer was first proposed by Choi [1]. Buongiorno [2] initially introduced nanofluid flow modelling, emphasizing the significance of thermophoresis and Brownian motion as key slip mechanisms in nanofluid. Recent investigations by Matta and Nagaraju [3], Gajjela et al. [4], Nagaraju et al. [5], Gajjela and Garvandha [6], Akaje et al. [7], Sharma et al. [8], Hattab et al. [9], Pati et al. [10,11] and Mishra et al. [12] highlight the growing interest in computational modelling and study of nanofluid flow with heat and mass transfer aspects.

The analysis of boundary layer flow with heat and mass transfer around a stretching cylinder has gained importance due to its relevance in industries such as thermal insulation, metal spinning, liquid film condensation and wire coating. Several researchers, including Crane [13], Lin and Shih [14], Wang [15], Rangi and Ahmad [16], have investigated the flow of Newtonian fluids, whereas Gajjela and Garvandha [17] examined the flow of couple stress fluid past a stretching cylinder, recognizing its practical significance. Numerous researchers have explored various physical aspects of nanofluid flow with heat and mass transfer over a stretching cylinder. For example, Sinha et al. [18] investigated the forced convection nanofluid flow around a stretching cylinder, while Bakar et al. [19] conducted stability analysis on nanofluid flow over a shrinking/stretching cylinder with suction effects. Khan et al. [20] examined MHD nanofluid flow around a stretching cylinder with thermal slip, radiation and blowing/suction. Mehmood et al. [21] studied electromagnetohydrodynamic nanofluid flow past a stretching cylinder containing alumina and ethylene glycol using convective boundary conditions. Mishra and Kumar [22] explored nanofluid MHD flow around a stretching cylinder, considering joule heating, viscous dissipation, velocity and thermal slip effects. Hussain and Malik [23] studied the MHD flow of a nanofluid past a stretching

cylinder with gyrotactic microorganisms under Nield conditions and convective boundary conditions. Singh et al. [24] investigated the non-uniform heat source and melting heat transfer of MHD copper water nanofluid flow over a porous stretching cylinder. Pattnaik et al. [25] examined the influences of non-linear radiation, homogeneous-heterogeneous reactions, heat source and magnetic field effects on nanofluid flow past a stretching cylinder in porous media. Alqahtani et al. [26] studied the impact of viscous dissipation and thermal radiation on nanofluid flow over a stretching/shrinking cylinder. Muhammad et al. [27] developed a mathematical model for CNT-water mixed convective nanofluid flow past a stretching cylinder. Elbashbeshy et al. [28] examined the influences of heat absorption/generation on nanofluid flow across an inclined stretching cylinder with gyrotactic microorganisms. Othman et al. [29] examined the influences of buoyancy force, heat absorption/generation, chemical reaction and activation energy on nanofluid flow past an inclined stretching cylinder with gyrotactic microorganisms. Pashikanti and Priyadharshini [30] analyzed the viscous dissipation, magnetic fields and slip effects on nanofluid flow past a stretching cylinder. Vinita et al. [31] examined the MHD and chemical reaction effects on nanofluid flow over a stretched cylinder. Makhdom et al. [32] investigated the effects of suction and joule heating on MHD stagnation point nanofluid flow past a horizontal cylinder. Mandal [33] analyzed the influences of viscous dissipation, chemical reaction and thermal radiation on MHD mixed convective nanofluid flow over a stretched cylinder. Recently, Boujelbene et al. [34] demonstrated the MHD and interface slip effects of nanofluid flow past a heated stretching cylinder. Saranya et al. [35] studied the effects of homogeneous-heterogeneous reactions and heat generation on the MHD flow of a nanofluid past a contracting cylinder. Irfan and Bhatti [36] explored the slip effects on MHD nanofluid flow over a stretching cylinder in porous media.

Several researchers (Khan et al. [20]; Mehmood et al. [21]; Mishra and Kumar [22]; Hussain and Malik [23]; Singh et al. [24]; Pattnaik et al. [25]; Pashikanti and Priyadharshini [30]; Vinita et al. [31]; Makhdom et al. [32]; Mandal [33]; Boujelbene et al. [34]; Saranya et al. [35]; Irfan and Bhatti [36]) have examined the magnetohydrodynamic (MHD) nanofluid flow. In all the previously mentioned magnetohydrodynamic (MHD) flows, the base fluid is assumed to be electrically conductive, and the influence of electrified nanoparticles resulting from triboelectrification, induced by the collision of nanoparticles due to Brownian motion, is not taken into account. However, the interaction between solid particles and the fluid is significantly influenced by a small static charge on the solid particles, as highlighted by Loeb [37] and Soo [38]. Also, Misra et al. [39] examined the effect of the electrification of particles on heat transfer in a two-phase boundary layer flow past a semi-infinite flat plate and concluded that the electrification of particles significantly

affects the heat transfer. Additionally, Kang and Wang [40] determined that molecular collisions occur between the fluid and nanoparticles due to electrostatic forces, which primarily enhance heat transfer in nanofluids. In recent years, some investigations into nanofluid flow coupled with nanoparticle electrification have been conducted for different geometries. Pattnaik et al. [41] examined the impact of nanoparticle electrification on natural convective nanofluid flow with internal heat generation. Pati et al. [42] investigated the effects of nanoparticle electrification on heat and mass transfer in natural convective nanofluid flow over a vertical flat plate with Brownian motion and thermophoresis. Panda et al. [43] explored the effects of electrified nanoparticles and viscous dissipation on the flow of Al_2O_3 -water nanofluid along a stretching sheet. Pattnaik et al. [44] studied the effects of nanoparticle electrification on heat and mass transfer in Cu-water nanofluid flow over an exponentially stretching surface in the presence of viscous dissipation, thermophoresis and Brownian motion. Recently, Pati et al. [45] examined the effects of nanoparticle electrification and the electric Reynolds number on the flow of a nanofluid along a vertical plane surface.

After an extensive review of the existing literature, it is observed that the combined effects of electrified nanoparticles and viscous dissipation on the flow of Ag-water nanofluid around a stretching cylinder have not yet been investigated. The current study introduces a novel exploration into the impact of nanoparticle electrification and viscous dissipation mechanisms on the heat and mass transfer characteristics of Ag-water nanofluid flow past a stretching cylinder, employing Buongiorno's two-component model. The flow analysis is mathematically modelled using a

system of nonlinear partial differential equations (PDEs), which are subsequently transformed into a dimensionless set of local similarity equations via similarity substitutions. The resulting local similarity equations are solved numerically using the MATLAB bvp4c solver, and the computed results are presented graphically for detailed analysis.

MATHEMATICAL FORMULATION

The present analysis examines the steady, incompressible, axisymmetric laminar boundary layer nanofluid flow, wherein the nanoparticles are charged. The flow is generated by a horizontally stretching cylinder located at $r = a$ with a fixed origin O. The cylinder undergoes extension with a stretching velocity $U_w = \frac{U_0 z}{l}$ along the z -axis. Here l is the characteristic length. At the cylinder surface, the nanoparticle concentration C_w and wall temperature T_w remain constant. Ambient values of nanoparticle concentration and temperature, denoted as C_∞ and T_∞ respectively, prevail as r tends to infinity. It is assumed that T_w and C_w exceed T_∞ and C_∞ respectively. The geometry of the investigation is illustrated in Figure 1.

The governing equations of nanofluid (Buongiorno [2], Pati et al. [45,46]) with viscous dissipation and electrified nanoparticles are formulated as follows:

$$\frac{\partial}{\partial r}(rv) + \frac{\partial}{\partial z}(ru) = 0, \quad (1)$$

$$v \frac{\partial u}{\partial r} + u \frac{\partial u}{\partial z} = \frac{\rho_s}{\rho_{nf}} \left(\frac{q}{m} \right) (C - C_\infty) E_z + \frac{\mu_{nf}}{\rho_{nf}} \left(\frac{\partial^2 u}{\partial r^2} + \frac{1}{r} \frac{\partial u}{\partial r} \right), \quad (2)$$

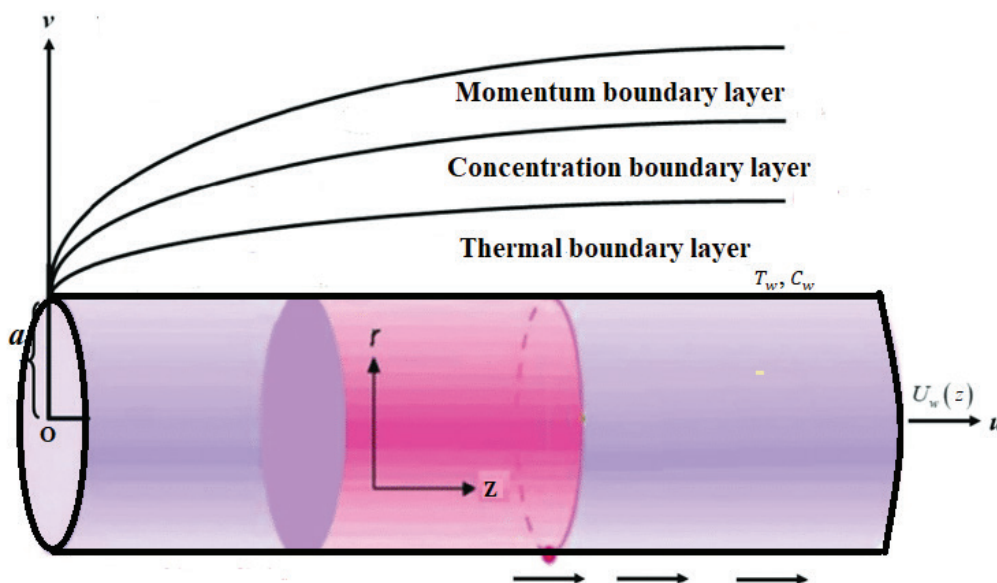


Figure 1. Geometry of the study.

$$(\rho c)_{nf} \left(v \frac{\partial T}{\partial r} + u \frac{\partial T}{\partial z} \right) = (\rho c)_s \frac{c}{Fm} \left(E_r \frac{\partial T}{\partial r} + E_z \frac{\partial T}{\partial z} \right) + \mu_{nf} \left(\frac{\partial u}{\partial r} \right)^2 + (\rho c)_s \left[D_B \frac{\partial C}{\partial r} \frac{\partial T}{\partial r} + \frac{D_T}{T_\infty} \left(\frac{\partial T}{\partial r} \right)^2 \right] + k_{nf} \left(\frac{\partial^2 T}{\partial r^2} + \frac{1}{r} \frac{\partial T}{\partial r} \right), \quad (3)$$

$$\left(v \frac{\partial C}{\partial r} + u \frac{\partial C}{\partial z} \right) = \left(\frac{q}{m} \right)_s \frac{1}{F} \left[\frac{\partial}{\partial z} (C E_z) + \frac{1}{r} \frac{\partial}{\partial r} (r C E_r) \right] + D_B \left(\frac{\partial^2 C}{\partial r^2} + \frac{1}{r} \frac{\partial C}{\partial r} \right) + \frac{D_T}{T_\infty} \left(\frac{\partial^2 T}{\partial r^2} + \frac{1}{r} \frac{\partial T}{\partial r} \right). \quad (4)$$

The boundary conditions of the flow are presented as:

$$\left. \begin{aligned} u = U_W(z) = \frac{U_0 z}{l}, v = 0, T = T_w, C = C_w \text{ at } r = a, \\ u \rightarrow U_\infty(z) = 0, T \rightarrow T_\infty, C \rightarrow C_\infty \text{ as } r \rightarrow \infty. \end{aligned} \right\} \quad (5)$$

Where, a is the radius of the cylinder. The components of velocity are denoted by u and v , while E_z and E_r denote the components of electric intensity along the z and r axes, respectively.

Using the set of similarity transformation $\eta = \frac{r^2 - a^2}{2a} \sqrt{\frac{U_0}{\nu_f}}$, $\psi = a \sqrt{\frac{\nu_f U_0}{l}} z f(\eta)$, $\theta(\eta) = \frac{T - T_\infty}{T_w - T_\infty}$, $s(\eta) = \frac{C - C_\infty}{C_w - C_\infty}$, equation (1) is clearly satisfied and the equations (2) to (4) are converted into locally similarity equations as follows:

$$f'''' + \frac{\varphi_1 \varphi_2}{(1+2\gamma\eta)} \frac{M Sc Nb}{N_F} s - \frac{\varphi_1}{(1+2\gamma\eta)} \left[f'^2 - f f'' - \frac{2}{\varphi_1} \gamma f''' \right] = 0, \quad (6)$$

$$\theta'' + \frac{Pr}{\varphi_4} \left[Nb \theta' s' + \frac{1}{2\gamma} \frac{Sc N_F Nb}{N_{Re}} (s + Nc) \theta' + Nt (\theta')^2 + \varphi_5 Ec (f'')^2 \right] + \frac{1}{(1+2\gamma\eta)} \left[2\gamma \theta' + \frac{Pr}{\varphi_3 \varphi_4} f \theta' \right] = 0, \quad (7)$$

$$s'' + \frac{1}{(1+2\gamma\eta)} \left[2\gamma s' + \frac{N_F Sc}{N_{Re}} \left(\frac{1}{2\gamma} s' + \eta s' + s + Nc \right) + Sc f s' + 2 \frac{Nt}{Nb} \gamma \theta' \right] + \frac{Nt}{Nb} \theta'' = 0, \quad (8)$$

with the dimensionless boundary conditions:

$$\left. \begin{aligned} \eta = 0, f(0) = 0, f'(0) = 1, \theta(0) = s(0) = 1, \\ \eta \rightarrow \infty, \theta(\infty) \rightarrow 0, s(\infty) \rightarrow 0, f'(\infty) \rightarrow 0. \end{aligned} \right\} \quad (9)$$

Here prime denotes derivative with respect to η . The dimensionless parameters are presented as follows:

$$\begin{aligned} \gamma &= \frac{1}{a} \sqrt{\frac{\nu_f l}{U_0}}, 1 + 2\gamma\eta = 1 + 2 \frac{1}{a} \sqrt{\frac{\nu_f l}{U_0}} \frac{r^2 - a^2}{2a} \sqrt{\frac{U_0}{\nu_f}} = 1 + \frac{r^2 - a^2}{a^2} = \frac{r^2}{a^2}, \\ Nt &= \frac{\rho_s c_s D_T (T_w - T_\infty)}{\rho_f c_f T_\infty \nu_f}, Nb = \frac{\rho_s c_s (C_w - C_\infty) D_B}{\rho_f c_f \nu_f}, M = \frac{q}{m} \frac{1}{F U_W} E_z, \\ N_F &= \frac{U_W}{F z}, \frac{1}{N_{Re}} = \left(\frac{q}{m} \right)^2 \frac{\rho_s}{\epsilon_0 (U_W)^2}, Sc = \frac{\nu_f}{D_B}, Nc = \frac{C_\infty}{(C_w - C_\infty)}, \\ Ec &= \frac{(U_W)^2}{(T_w - T_\infty) c_f}, Pr = \frac{\nu_f}{\alpha_f}. \end{aligned}$$

And the thermophysical constants (Maharukh et al. [47]) are defined as follows:

$$\begin{aligned} \varphi_1 &= (1 - C_\infty)^{2.5} \left[C_\infty \frac{\rho_s}{\rho_f} + (1 - C_\infty) \right], \\ \varphi_2 &= \frac{c_f}{c_s} \frac{1}{\left[C_\infty \frac{\rho_s}{\rho_f} + (1 - C_\infty) \right]}, \\ \tau &= \frac{(\rho c)_s}{(\rho c)_f}, \varphi_3 = \frac{1}{C_\infty \tau + (1 - C_\infty)}, \\ \varphi_4 &= \frac{k_s + 2k_f - 2C_\infty(k_f - k_s)}{k_s + 2k_f + C_\infty(k_f - k_s)}, \\ \varphi_5 &= \frac{1}{(1 - C_\infty)^{2.5}}. \end{aligned}$$

The investigation utilizes a nanofluid comprising a 1% concentration of silver (Ag) nanoparticles in comparison to pure water, with $Pr = 6.2$. The thermophysical characteristics of both pure water and silver are referenced from Upreti et al. [48], as presented in Table 1.

Table 1. Thermophysical characteristics

Property	Ag	Pure water
c (J/kgK)	235	4179
ρ (kg/m ³)	10,500	997.1
k (W/mK)	429	0.613

In the realm of heat and mass transfer applications, the significance lies in the local Nusselt number (Nu_z) and the local Sherwood number (Sh_z), both of which are defined as follows for practical purposes.

$$\begin{aligned} Nu_z &= \frac{z q_w}{k_f (T_w - T_\infty)}, \text{ where } q_w = -k_f \left(\frac{\partial T}{\partial r} \right)_{r=a}, \\ Sh_z &= \frac{z q_m}{D_B (C_w - C_\infty)}, \text{ where } q_m = -D_B \left(\frac{\partial C}{\partial r} \right)_{r=a}. \end{aligned}$$

The skin friction coefficient is defined as follows:

$$C_f = \frac{\tau_w}{\rho_f U_W^2}, \text{ where } \tau_w = \mu_f \left(\frac{\partial u}{\partial r} \right)_{r=a}.$$

The dimensionless, skin friction coefficient ($f''(0)$), reduced Nusselt number ($-\theta'(0)$) and reduced Sherwood number ($-s'(0)$) are formulated as follows:

$$\begin{aligned} f''(0) &= C_f (Re_z)^{1/2}, \\ -\theta'(0) &= Nu_z (Re_z)^{-1/2}, \\ -s'(0) &= Sh_z (Re_z)^{-1/2}, \end{aligned}$$

where $Re_z = \frac{U_0 z^2}{\nu_f l}$.

Method of Solution

The local similarity method emerges as the preferred approach among various methods due to its straightforward conceptual and computational ease in addressing 2-D problems lacking similarity solutions. With this method, non-similar solutions at specific streamwise stations can be obtained without the need to solve for other streamwise stations, which is a noteworthy advantage. Additionally, the governing equations resemble calculus-like ordinary differential equations (ODEs), enhancing the appeal of this strategy. Further elaboration on this technique can be found in the following references: Farooq et al. [49], Usman et al. [50], Maji and Sahu [51], and Lund et al. [52].

The equations (6) to (8) exhibit characteristics of local similarity equations, as the parameters $N_F = N_F(z)$ and $N_{Re} = N_{Re}(z)$ solely involve variables. Since the parameters are still contingent upon the independent variable z , numerical solutions remain valid, offering a local similarity solution. The MATLAB software's `bvp4c` solver is employed for solving the local similarity equations (6) to (8) with non-dimensional boundary conditions (9). Achieving highly accurate solutions necessitates careful selection and fine-tuning of initial estimates, other parameter values, and optimal boundary layer thickness within the solver's coding framework. It's crucial to highlight that Figures 2-8 illustrate the results, presenting numerical solutions for dimensionless velocity, temperature, and concentration profiles that meet the defined far stream boundary conditions (9). This helps validate the precision of the numerical findings obtained in this study.

COMPARISON AND VALIDATION STUDY

The impact of electrified nanoparticles and viscous dissipation on the heat and mass transfer properties of

Table 2. Comparison of dimensionless skin friction coefficient results

γ	$f''(0)$ (Rangi and Ahmad [16])	$f''(0)$ (present results)
0.00	-1.000000	-1.000001
0.50	-1.188715	-1.188723
1.00	-1.459308	-1.459330

Ag-Water nanofluid flow past a stretching cylinder has been investigated numerically. Table 2 displays the existing numerical results for regular fluids in the limiting scenario, as reported by Rangi and Ahmad [16], for different values of γ . Table 2 displays the outcomes, demonstrating strong alignment with the current findings, thereby ensuring the precision of the numerical results acquired in the present analysis.

RESULTS AND DISCUSSION

Numerical solutions were derived to examine the impacts of the electrification parameter (M) and Eckert number (Ec) on various non-dimensional variables, including velocity ($f'(\eta)$), temperature ($\theta(\eta)$), concentration $s(\eta)$, heat transfer coefficient ($-\theta'(0)$) and mass transfer coefficient ($-s'(0)$), with the remaining parameters held constant. The findings are visually represented in Figures 3 to 12. Additionally, Figure 2 displays the distributions of $f'(\eta)$, $\theta(\eta)$ and $s(\eta)$ that satisfy the non-dimensional far stream boundary conditions (9) asymptotically. It is observed that the thickness of the momentum boundary layer is greater compared to the thermal and concentration boundary layer thicknesses.

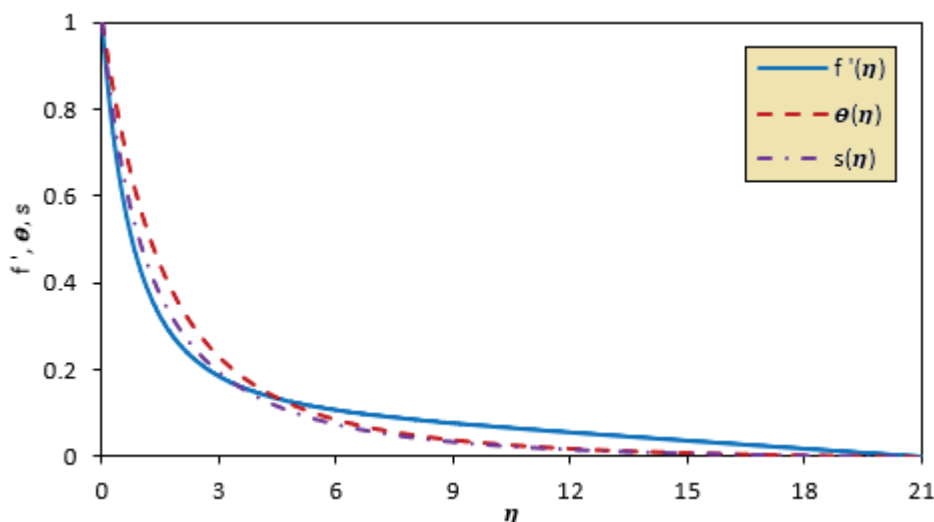


Figure 2. Plots of $f'(\eta)$, $\theta(\eta)$ and $s(\eta)$ for the case

$$N_F = M = Ec = Nb = Nt = Nc = 0.1, \gamma = 0.5, Pr = 6.2, \\ Sc = N_{Re} = 2.0.$$

The effect of M on $f'(\eta)$ is depicted in Figure 3. It is observed that as M increases, both the velocity and thickness

of the momentum boundary layer increase. A rise in M leads to an amplification of the drag force on ions, which in turn exerts an equal and opposite reaction force on neutral fluid molecules. This mechanism results in an increase in

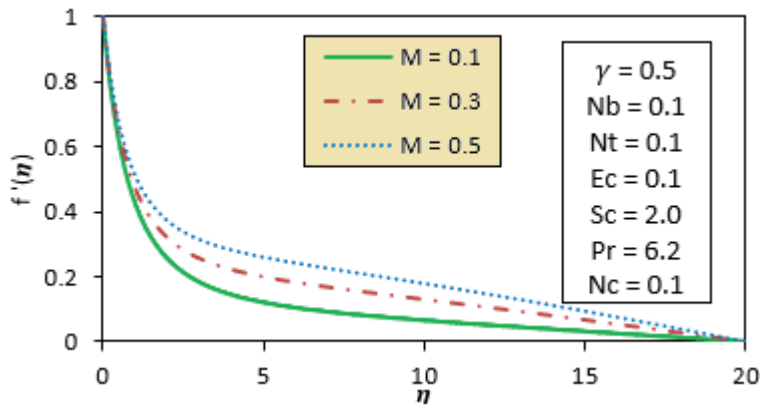


Figure 3. Variation of $f'(\eta)$ with M when $N_{Re} = 2.0, N_F = 0.1$.

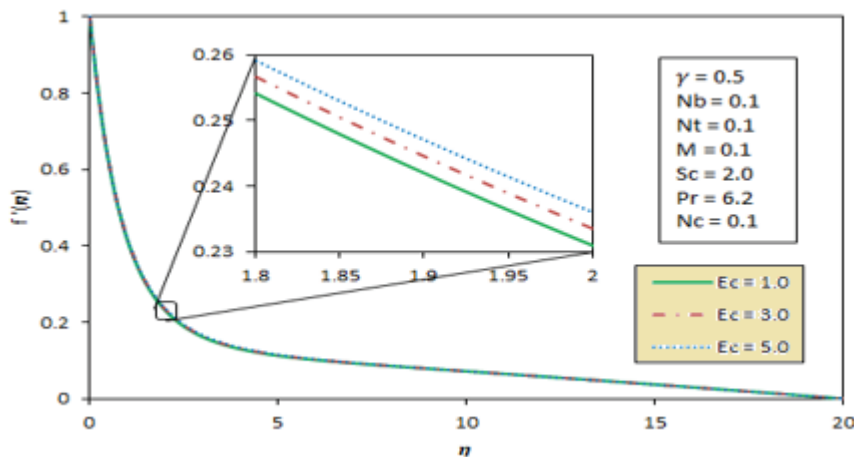


Figure 4. Variation of $f'(\eta)$ with Ec when $N_{Re} = 2.0, N_F = 0.1$.

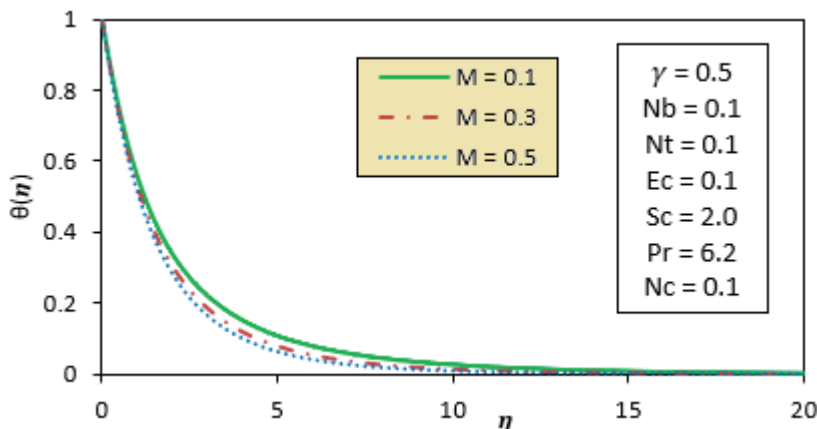


Figure 5. Variation of $\theta(\eta)$ with M when $N_{Re} = 2.0, N_F = 0.1$.

$f'(\eta)$. Figure 4 shows that an increase in Ec results in a slight increase in the velocity profile within the boundary layer, attributed to the increase in stretching velocity associated with the increment of Ec .

The impact of M on $\theta(\eta)$ is illustrated in Figure 5. Increasing M leads to a reduction in both $\theta(\eta)$ and the thickness of the thermal boundary layer. This is because higher M results in increased fluid velocity, causing hotter fluid particles to move away and thus lowering $\theta(\eta)$. Conversely, higher values of Ec , as depicted in Figure 6, lead to an increase in $\theta(\eta)$. This is due to viscous dissipation generating heat through drag between fluid particles, thereby raising the fluid temperature.

Figure 7 examines the influence of M on $s(\eta)$. Both the thickness of the concentration boundary layer and $s(\eta)$ decrease as M increases. This is because as M increases, nanoparticles migrate from the fluid region toward the cylinder, resulting in a decrease in $s(\eta)$ and the corresponding boundary layer thickness. Figure 8

illustrates the effect of Ec on $s(\eta)$. Near the surface of the cylinder, there is a gradual decrease in $s(\eta)$, whereas a contrasting pattern is observed farther away from the cylinder for higher values of Ec . This is attributed to conduction heat transfer surpassing convection heat transfer near the cylinder.

The effect of M on the dimensionless heat transfer coefficient $-\theta'(0)$ and the dimensionless mass transfer coefficient $-s'(0)$ is depicted in Figures 9 and 10, respectively. It is observed that as M increases, the rates of heat and mass transfer improve for different values of Nb . This improvement occurs because the dimensionless temperature and concentration decrease near the surface of the stretching cylinder with increasing values of M . Consequently, this reduction enhances the rates of both heat and mass transfer from the cylinder surface to the nanofluid. The values $N_F = Ec = Nt = Nc = 0.1$, $\gamma = 0.5$, $Pr = 6.2$, $Sc = N_{Re} = 2.0$ remain constant across all the findings depicted in Figures 9 and 10. Figures 11 and 12 illustrate the impact of Ec on

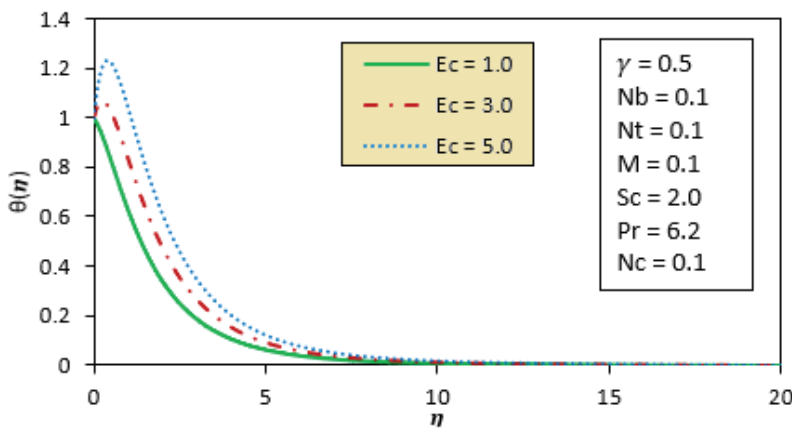


Figure 6. Variation of $\theta(\eta)$ with Ec when $N_{Re} = 2.0$, $N_F = 0.1$.

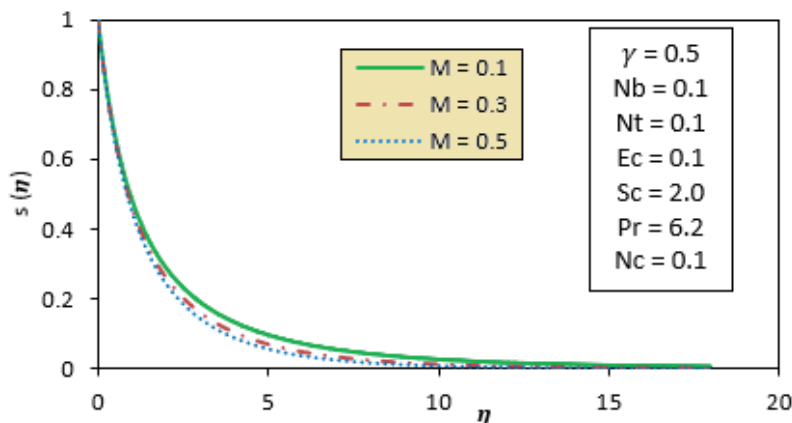


Figure 7. Variation of $s(\eta)$ with M when $N_{Re} = 2.0$, $N_F = 0.1$.

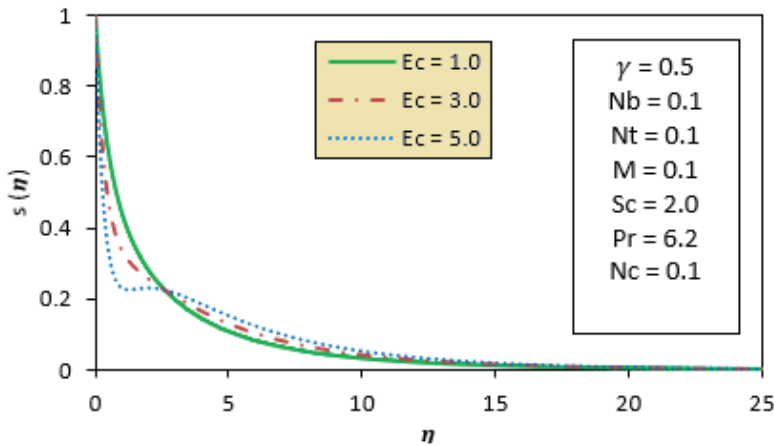


Figure 8. Variation of $s(\eta)$ with Ec when $N_{Re} = 2.0$, $N_F = 0.1$.

$-\theta'(0)$ and $-s'(0)$, respectively. As the Eckert number (Ec) increases, it is observed that heat transfer rates reduce while mass transfer rates enhance across different Brownian motion parameter (Nb) values. This change occurs because the dimensionless temperature increases and the dimensionless concentration decreases near the surface of the stretching cylinder as Ec values increase, leading to reduced heat transfer rates and enhanced mass transfer rates. The parameters $N_F = M = Nt = Nc = 0.1$, $\gamma = 0.5$, $Pr = 6.2$, $Sc = N_{Re} = 2.0$ remain constant throughout the findings presented in Figures 11 and 12. Additionally, it is noticed that $-\theta'(0)$ monotonically lessens whereas $-s'(0)$ boosts with a climb in Brownian motion parameter (Nb).

Figures 13 and 14 depict the streamline patterns of nanofluid under different electrification parameter values. As M increases, the nanofluid streamlines become more constricted. Moreover, the presence of electrified nanoparticles

yields more pronounced streamline patterns compared to scenarios without electrification. Figures 15 and 16 illustrate the contour distributions for $-\theta'(0)$ and $-s'(0)$ as the electrification parameter (M) and Eckert number (Ec) increase. An increase in M consistently leads to a rise in $-\theta'(0)$, although this trend is reversed at higher Ec values as shown in Figure 15. The enhancement in $-\theta'(0)$ is due to a decrease in the dimensionless temperature near the surface of the stretching cylinder as the value of M increases. Conversely, the reduction in $-\theta'(0)$ happens because the dimensionless temperature near the surface of the stretching cylinder rises with increasing Ec values. Additionally, Figure 16 demonstrates that $-s'(0)$ significantly improves with the growth of both M and Ec . The increase in $-s'(0)$ occurs due to a reduction in the dimensionless concentration near the surface of the stretching cylinder as the values of both M and Ec rise.

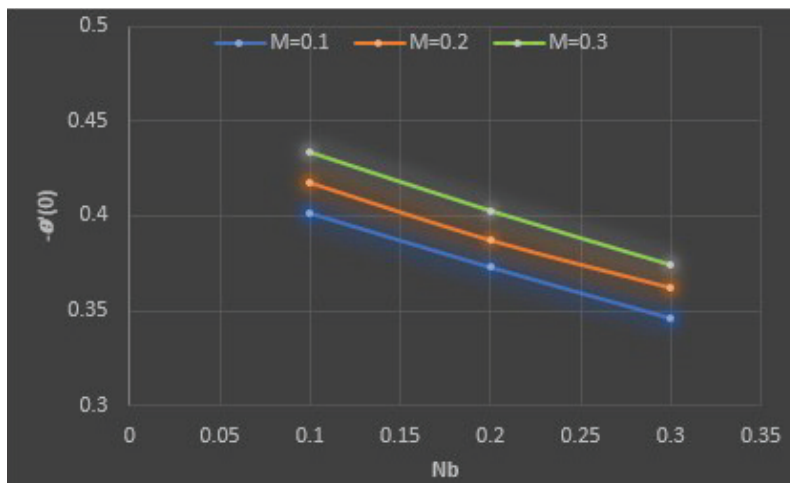


Figure 9. Effect of M on $-\theta'(0)$.

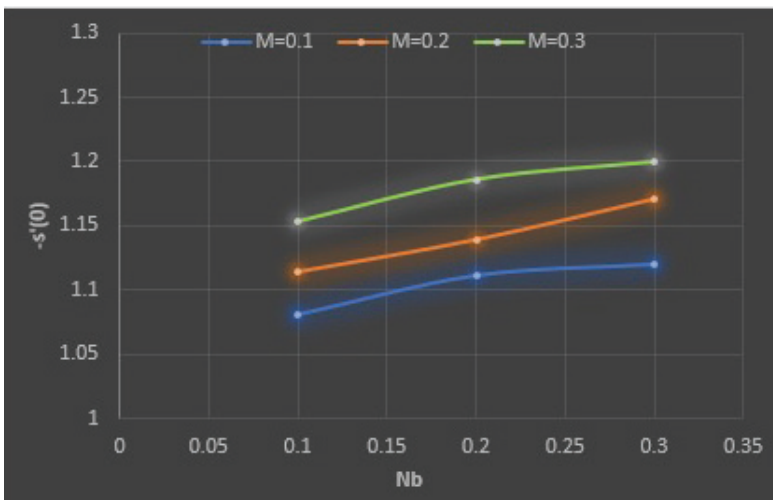


Figure 10. Effect of M on $-s'(0)$.

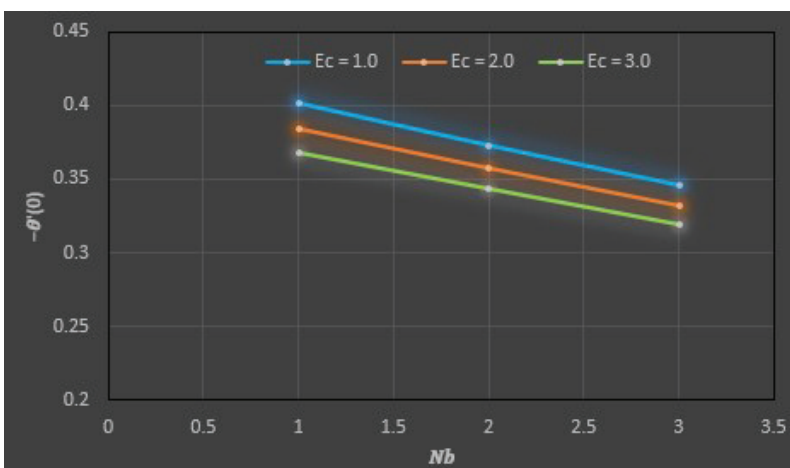


Figure 11. Effect of Ec on $-\theta'(0)$.

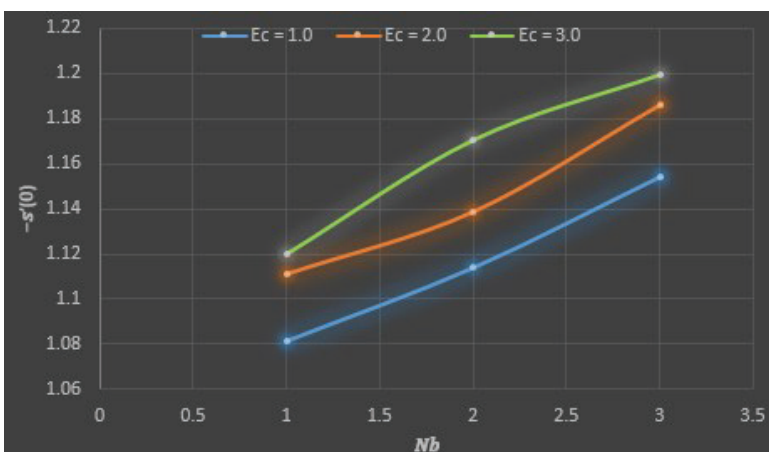


Figure 12. Effect of Ec on $-s'(0)$.

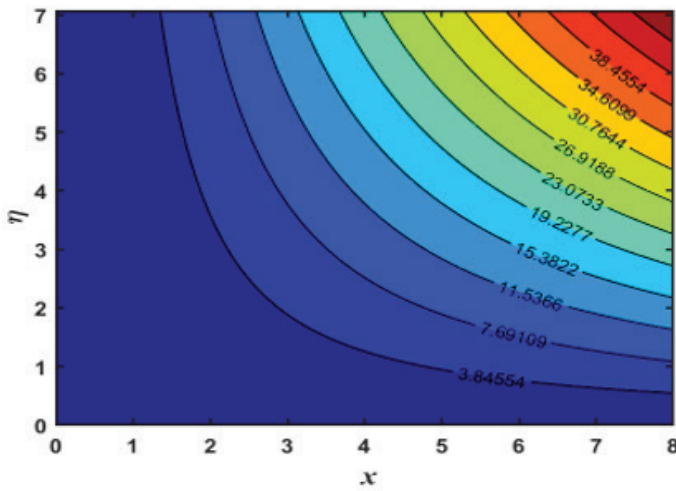


Figure 13. Effect of electrification parameter ($M = 0$) on streamlines.

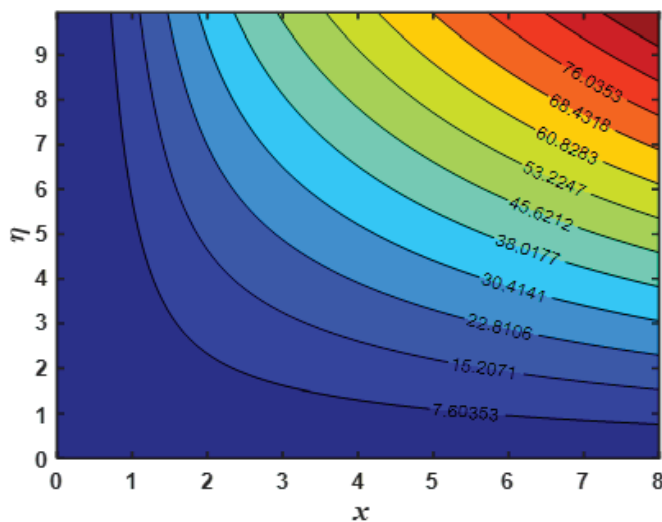


Figure 14. Effect of electrification parameter ($M = 0.2$) on streamlines.

CONCLUSION

The study delves into the mathematical modelling of boundary layer Ag-water nanofluid flow around a stretching cylinder, exploring the impact of M and Ec on $f'(\eta)$, $\theta(\eta)$, $s(\eta)$, $-\theta'(0)$ and $-s'(0)$. The numerical investigation focuses on studying the variations of $-\theta'(0)$ and $-s'(0)$ concerning the values of M and Ec , with the results presented graphically. The analysis of these findings yields the following conclusions:

- As the electrification parameter M rises, the non-dimensional velocity experiences growth, while the dimensionless concentration and temperature decrease within the boundary layer region.
- As the Eckert number Ec increases, there is an increase in the non-dimensional velocity and temperature, while the dimensionless concentration exhibits a dual nature.
- An increase in the electrification parameter M enhances the rate of heat transfer from the stretching cylinder to the nanofluid. This enhancement in heat transfer due to nanoparticle electrification facilitates the dissipation of heat into the cooler nanofluid, effectively cooling the stretching cylinder. This improved heat transfer property of nanofluid due to the electrified nanoparticle mechanism is particularly beneficial in manufacturing industries that produce cylindrical-shaped products, where the temperature of these products is significantly high during the manufacturing process. By promoting efficient heat transfer, the electrification of

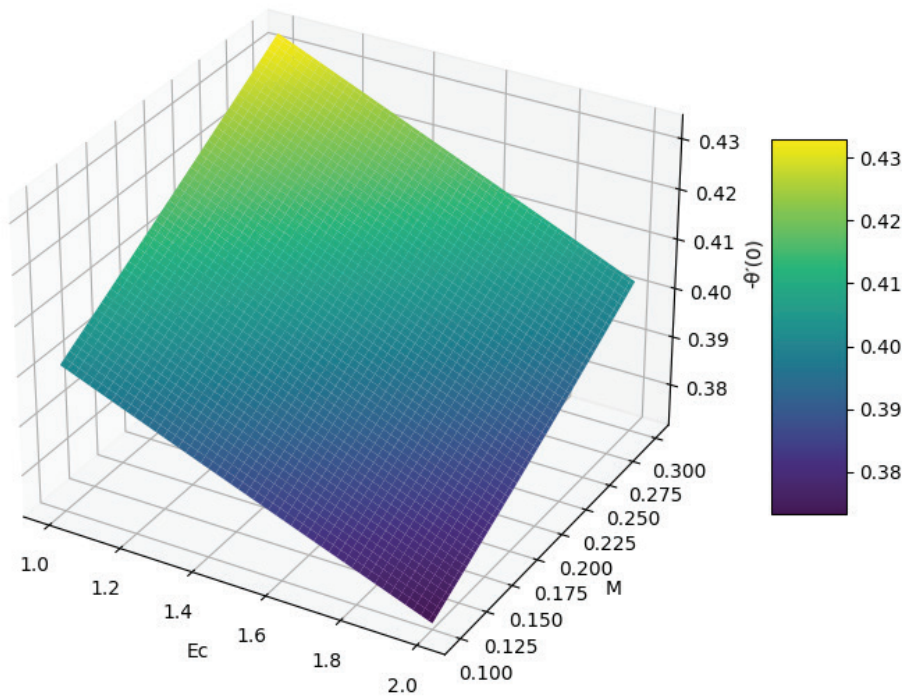


Figure 15. Contour plot for variation of dimensionless heat transfer coefficient with M and Ec .

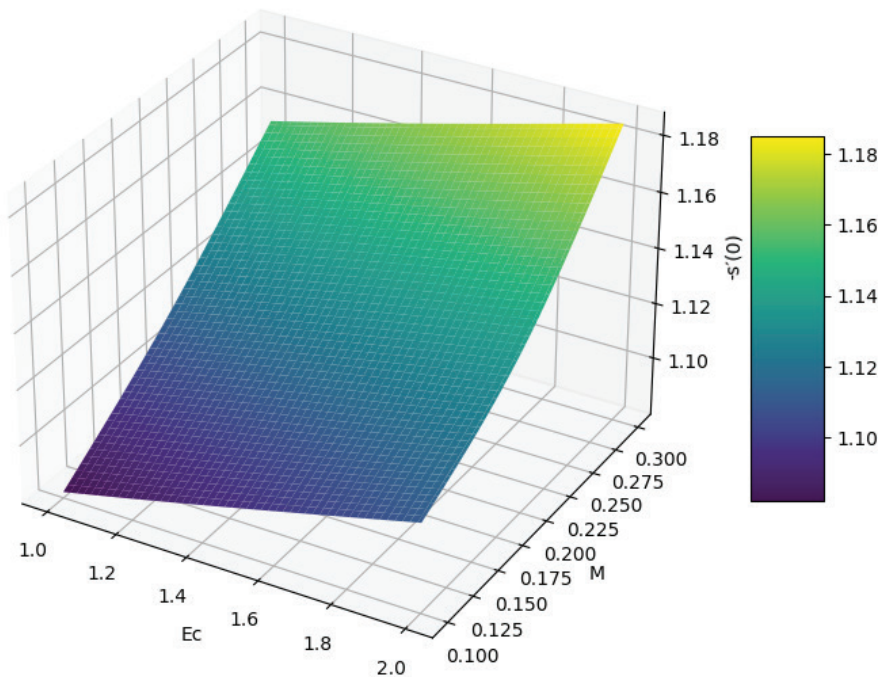


Figure 16. Contour plot for variation of dimensionless mass transfer coefficient with M and Ec .

nanoparticles helps in managing and reducing the temperature of the products, thereby improving the overall manufacturing efficiency and product quality.

- The increase in the electrification parameter M increases the mass transfer rate from the stretching cylinder to

the nanofluid. This improvement in mass transfer is due to the enhanced mobility and distribution of nanoparticles within the nanofluid under the influence of electrification. The electrification mechanism significantly enhances the transport properties of the nanofluid,

which can be particularly beneficial in biomedical applications. In such applications, the enhanced mass transfer can improve the efficacy of drug delivery systems. The nanoparticles, which serve as carriers for therapeutic agents, are more effectively distributed and transported to targeted areas within the body.

- An increase in the Eckert number Ec results in enhanced mass transfer rates while causing a decline in heat transfer rates from the cylindrical surface to the nanofluid.
- The inclusion of the nanoparticle electrification mechanism significantly impacts the stream lines of the flow.

The incorporation of electrified nanoparticles emerges as a crucial factor in the modelling of Ag-water nanofluid flow driven by a horizontally stretched cylinder. This mechanism plays a significant role in enhancing both heat and mass transfer aspects of the Ag-water nanofluid flow.

NOMENCLATURE

c	specific heat capacity
C	nanoparticles volume concentration
D_B	Brownian diffusion coefficient
D_T	thermophoresis diffusion coefficient
Ec	Eckert number
f	non-dimensional stream function
F	time constant for momentum transfer between the fluid and nanoparticles
g	gravitational acceleration
k	thermal conductivity
m	nanoparticle mass
M	electrification parameter
Nb	Brownian motion parameter
Nc	concentration ratio
N_F	momentum transfer number
N_{Re}	electric Reynolds number
Nt	thermophoresis parameter
Nu_z	local Nusselt number
Pr	Prandtl number
q	charge of the nanoparticle
q_w	wall heat flux
q_m	wall mass flux
Re_z	local Reynolds number
s	non-dimensional concentration
Sc	Schmidt number
Sh_z	local Sherwood number
T	temperature
(z,r)	cylindrical polar coordinates

Greek Symbols

α	thermal diffusivity
γ	curvature parameter
η	similarity variable
μ	dynamic viscosity
θ	temperature in dimensionless form
ρ	density
τ_w	wall shear stress

ν	kinematic viscosity
ψ	stream function

Subscripts

s	nanoparticles
nf	nanofluid
f	base fluid
w	condition at the cylinder surface
∞	ambient values

ACKNOWLEDGEMENTS

The authors express their gratitude to the anonymous referees for their insightful suggestions and constructive feedback, which significantly enhanced the quality of the paper.

AUTHORSHIP CONTRIBUTIONS

AKP formulated the mathematical model, generated the numerical results, and wrote the manuscript. AM performed the literature review, while SKM developed the MATLAB bvp4c code for the problem.

DATA AVAILABILITY STATEMENT

The authors confirm that the data that supports the findings of this study are available within the article. Raw data that support the finding of this study are available from the corresponding author, upon reasonable request.

CONFLICT OF INTEREST

The author declared no potential conflicts of interest with respect to the research, authorship, and/or publication of this article.

ETHICS

There are no ethical issues with the publication of this manuscript.

REFERENCES

- [1] Sus C. Enhancing thermal conductivity of fluids with nanoparticles, developments and applications of non-Newtonian flows. ASME FED MD 1995;231:99–105.
- [2] Buongiorno J. Convective transport in nanofluids. J Heat Transf 2006;128:240–250. [CrossRef]
- [3] Matta A, Nagaraju G. The influence of double diffusive gradient boundary condition on micropolar nano fluid flow through stretching surface with a higher order chemical reaction. Int J Comput Sci Math 2021;14:301–313. [CrossRef]
- [4] Gajjela N, Garvandha M, Kumar D. Heat transfer in couple stress two-fluid flow model: Effects of modified heat flux, electromagnetic force, and uneven heat source/sink. Comput Therm Sci 2023;15:1–14. [CrossRef]

- [5] Nagaraju G, Shilpa S, Naresh Kumar N. Entropy generation analysis of a magnetized $\text{Al}_2\text{O}_3\text{-H}_2\text{O}$ nanofluid between viscous heating horizontal internal rotating annulus and Joule heating. *Int J Math Comput Res* 2019;7:1973–1983.
- [6] Gajjela N, Garvandha M. Impacts of variable thermal conductivity and mixed convective stagnation-point flow in a couple stress nanofluid with viscous heating and heat source. *Heat Transf* 2020;49:3630–3650. [\[CrossRef\]](#)
- [7] Akaje TW, Olajuwon BI, Musiliu Tayo RAJI. Computational analysis of the heat and mass transfer in a casson nanofluid with a variable inclined magnetic field. *Sigma* 2023;41:512–523. [\[CrossRef\]](#)
- [8] Sharma R, Aruna D, Mishra MK, Sinha SB. Scrutiny of flow and heat transfer characteristics of hybrid nanofluid passing through a squeezing channel. *Sigma J Eng Nat Sci* 2024;42:1856–1865. [\[CrossRef\]](#)
- [9] El Hattab M, Boumhaout M, Oukach S. MHD natural convection in a square enclosure using carbon nanotube–water nanofluid with two isothermal fins. *Sigma J Eng Nat Sci* 2024;42:1075–1087. [\[CrossRef\]](#)
- [10] Pati AK, Rout MM, Sahu R, Ramakoti IS, Panda KK, Sethi KC. Chemical reaction, electrification, Brownian motion and thermophoresis effects of copper nanoparticles on nanofluid flow with skin friction, heat and mass transfer. *East Eur J Phys* 2024;4:152–158. [\[CrossRef\]](#)
- [11] Pati AK, Misra A, Mishra SK. Modeling electrification of nanoparticles in free convective nanofluid flow. *Test Eng Manag* 2020;83:17663–17669.
- [12] Mishra S, Pati AK, Misra A, Mishra SK. Thermal performance of nanofluid flow along an isothermal vertical plate with velocity, thermal, and concentration slip boundary conditions employing Buongiorno's revised non-homogeneous model. *East Eur J Phys* 2024;4:98–106. [\[CrossRef\]](#)
- [13] Crane LJ. Boundary layer flow due to a stretching cylinder. *Z Angew Math Phys* 1975;26:619–622. [\[CrossRef\]](#)
- [14] Lin HT, Shih YP. Laminar boundary layer along static and moving cylinders. *J Chin Inst Eng* 1980;3:73–79. [\[CrossRef\]](#)
- [15] Wang CY. Fluid flow due to a stretching cylinder. *Phys Fluids* 1988;31:466–468. [\[CrossRef\]](#)
- [16] Rangi RR, Ahmad N. Boundary layer flow past a stretching cylinder and heat transfer with variable thermal conductivity. *Appl Math* 2012;3:205–209. [\[CrossRef\]](#)
- [17] Gajjela N, Garvandha M. The influence of magnetized couple stress heat, and mass transfer flow in a stretching cylinder with convective boundary condition, cross-diffusion, and chemical reaction. *Therm Sci Eng Prog* 2020;18:100517. [\[CrossRef\]](#)
- [18] Sinha D, Jain P, Siddheshwar PG, Tomer NS. Forced convective flow of a nanofluid due to a stretching cylinder with free stream. *J Appl Fluid Mech* 2015;9:463–474. [\[CrossRef\]](#)
- [19] Bakar NAA, Bachok N, Arifin NM, Pop I. Stability analysis on the flow and heat transfer of nanofluid past a stretching/shrinking cylinder with suction effect. *Results Phys* 2018;9:1335–1344. [\[CrossRef\]](#)
- [20] Khan MI, Tamoor M, Hayat T, Alsaedi A. MHD boundary layer thermal slip flow by nonlinearly stretching cylinder with suction/blowing and radiation. *Results Phys* 2017;7:1207–1211. [\[CrossRef\]](#)
- [21] Mehmood OU, Maskeen MM, Zeeshan A. Electromagnetohydrodynamic transport of Al_2O_3 nanoparticles in ethylene glycol over a convectively heated stretching cylinder. *Adv Mech Eng* 2017;9:1687814017735282. [\[CrossRef\]](#)
- [22] Mishra A, Kumar M. Velocity and thermal slip effects on MHD nanofluid flow past a stretching cylinder with viscous dissipation and Joule heating. *SN Appl Sci* 2020;2:1350. [\[CrossRef\]](#)
- [23] Hussain A, Malik MY. MHD nanofluid flow over stretching cylinder with convective boundary conditions and Nield conditions in the presence of gyrotactic swimming microorganism: A biomathematical model. *Int Commun Heat Mass Transf* 2021;126:105425. [\[CrossRef\]](#)
- [24] Singh K, Pandey AK, Kumar M. Melting heat transfer assessment on magnetic nanofluid flow past a porous stretching cylinder. *J Egypt Math Soc* 2021;29:1–14. [\[CrossRef\]](#)
- [25] Pattnaik PK, Mishra SR, Bég OA, Khan UF, Umavathi JC. Axisymmetric radiative titanium dioxide magnetic nanofluid flow on a stretching cylinder with homogeneous/heterogeneous reactions in Darcy-Forchheimer porous media: Intelligent nanocoating simulation. *Mater Sci Eng B* 2022;277:115589. [\[CrossRef\]](#)
- [26] Alqahtani AM, Khan MR, Akkurt N, Puneeth V, Alhowaity A, Hamam H. Thermal analysis of a radiative nanofluid over a stretching/shrinking cylinder with viscous dissipation. *Chem Phys Lett* 2022;808:140133. [\[CrossRef\]](#)
- [27] Muhammad K, Hayat T. OHAM analysis of Newtonian heating in mixed convective flow of CNTs over a stretched cylinder. *Alex Eng J* 2022;61:3697–3707. [\[CrossRef\]](#)
- [28] Elbashesy EM, Asker HG, Nagy B. The effects of heat generation absorption on boundary layer flow of a nanofluid containing gyrotactic microorganisms over an inclined stretching cylinder. *Ain Shams Eng J* 2022;13:101690. [\[CrossRef\]](#)
- [29] Othman HA, Ali B, Jubair S, Yahya Almusawa M, Aldin SM. Numerical simulation of the nanofluid flow consists of gyrotactic microorganism and subject to activation energy across an inclined stretching cylinder. *Sci Rep* 2023;13:7719. [\[CrossRef\]](#)
- [30] Pashikanti J, Susmitha Priyadarshini DR. Influence of magnetic field and viscous dissipation due to graphene oxide nanofluid slip flow on an isothermally stretching cylinder. *Pramana* 2023;97:94. [\[CrossRef\]](#)

- [31] Kumar P, Poply V. Mathematical modelling of magnetohydrodynamic nanofluid flow with chemically reactive species and outer velocity towards stretching cylinder. *J Nanofluids* 2023;12:1067–1073. [\[CrossRef\]](#)
- [32] Makhdoum BM, Mahmood Z, Khan U, Fadhl BM, Khan I, Eldin SM. Impact of suction with nanoparticles aggregation and joule heating on unsteady MHD stagnation point flow of nanofluids over horizontal cylinder. *Heliyon* 2023;9:e15012. Retraction in: *Heliyon* 2025;11:e42824. [\[CrossRef\]](#)
- [33] Mandal G. Entropy analysis on magneto-convective and chemically reactive nanofluids flow over a stretching cylinder in the presence of variable thermal conductivity and variable diffusivity. *J Nanofluids* 2023;12:819–831. [\[CrossRef\]](#)
- [34] Boujelbene M, Rehman S, Jazaa Y, Dhaou MH. Thermodynamics of hydromagnetic boundary layer flow of Prandtl nanofluid past a heated stretching cylindrical surface with interface slip. *J Taiwan Inst Chem Eng* 2024;155:105310. [\[CrossRef\]](#)
- [35] Saranya S, Ragupathi P, Al-Mdallal QM. Thermal and reactive effects in nanofluid flow around a contracting cylinder under magnetic field influence. *Int J Thermofluids* 2024;22:100710. [\[CrossRef\]](#)
- [36] Irfan M, Bhatti MM. Effects of Arrhenius kinetic on the magnetized nanofluid flow through a porous stretchable cylinder with slip conditions. *Energy Sources A Recovery Util Environ Effects* 2024;46:1979–1995. [\[CrossRef\]](#)
- [37] Loeb LB. Static electrification. Springer-Verlag; 1958. [\[CrossRef\]](#)
- [38] Soo SL. Effect of electrification on dynamics of a particulate system. *Ind Eng Chem Fundam* 1964;3:75–80. [\[CrossRef\]](#)
- [39] Misra A, Mishra SK, Prakash J. Modeling electrification of suspended particulate matter (SPM) in a two phase laminar boundary layer flow and heat transfer over a semi-infinite flat plate. *Int Commun Heat Mass Transf* 2011;38:1110–1118. [\[CrossRef\]](#)
- [40] Kang Z, Wang L. Effect of thermal-electric cross coupling on heat transport in nanofluids. *Energies* 2017;10:123. [\[CrossRef\]](#)
- [41] Pattnaik R, Misra A, Mishra SK. Effect of electrification on natural convection boundary layer flow of nanofluid past a vertical plate with heat generation. *JP J Heat Mass Transf* 2019;17:577–595. [\[CrossRef\]](#)
- [42] Pati AK, Misra A, Mishra SK. Heat and mass transfer analysis on natural convective boundary layer flow of a Cu-water nanofluid past a vertical flat plate with electrification of nanoparticles. *Adv Appl Fluid Mech* 2019;23:1–15. [\[CrossRef\]](#)
- [43] Panda S, Misra A, Mishra SK, Pati AK, Pradhan KK. Flow and heat transfer analysis of H₂O-Al₂O₃ nanofluid over a stretching surface with electrified nanoparticles and viscous dissipation. *Adv Dyn Syst Appl* 2021;16:1533–1545.
- [44] Pattnaik R, Misra A, Mishra SK, Kumar K, Pradhan SP, Pati AK. Thermal performance analysis of nanofluid past an exponentially stretching surface due to the electrification effect of nanoparticles. *Int J Difference Equ* 2021;16:189–203.
- [45] Pati AK, Mishra S, Misra A, Mishra SK. Heat and mass transport aspects of nanofluid flow towards a vertical flat surface influenced by electrified nanoparticles and electric reynolds number. *East Eur J Phys* 2024;2:234–241. [\[CrossRef\]](#)
- [46] Pati AK, Misra A, Mishra SK, Mishra S, Sahu R, Panda S. Computational modelling of heat and mass transfer optimization in copper water nanofluid flow with nanoparticle ionization. *JP J Heat Mass Transf* 2023;31:1–18. [\[CrossRef\]](#)
- [47] Mahrukh M, Kumar A, Gu S, Kamnis S, Gozali E. Modeling the effects of concentration of solid nanoparticles in liquid feedstock injection on high-velocity suspension flame spray process. *Ind Eng Chem Res* 2016;55:2556–2573. [\[CrossRef\]](#)
- [48] Upreti H, Pandey AK, Kumar M. MHD flow of Ag-water nanofluid over a flat porous plate with viscous-ohmic dissipation, suction/injection and heat generation/absorption. *Alex Eng J* 2018;57:1839–1847. [\[CrossRef\]](#)
- [49] Farooq U, Waqas H, Bariq A, Elagan SK, Fatima N, Imran M, et al. Local similar solution of magnetized hybrid nanofluid flow due to exponentially stretching/shrinking sheet. *BioNanoScience* 2024;14:368–379. [\[CrossRef\]](#)
- [50] Khan WA, Uddin N, Muhammad T. Heat and mass transport in an electrically conducting nanofluid flow over two-dimensional geometries. *Heliyon* 2023;9:18377. [\[CrossRef\]](#)
- [51] Maji S, Sahu AK. Numerical investigation of mixed convection boundary layer flow for nanofluids under quasilinearization technique. *SN Appl Sci* 2021;3:833. [\[CrossRef\]](#)
- [52] Lund AL, Ching DLC, Omar Z, Khan I, Nisar KS. Triple local similarity solutions of Darcy-Forchheimer magnetohydrodynamic (MHD) flow of micropolar nanofluid over an exponential shrinking surface: Stability analysis. *Coatings* 2019;9:527. [\[CrossRef\]](#)